

Sensitivity Improvements to Laser Sensor for Boron Nitride Erosion in Hall Thrusters

IEPC-2011-068

Presented at the 32nd International Electric Propulsion Conference,
Wiesbaden, Germany
September 11–15, 2011

Brian C. Lee,* Lei Tao,[†] Joshua M. Taylor[‡] and Azer P. Yalin[§]
Colorado State University, Fort Collins, CO, 80523, USA

and

Alec Gallimore[¶]
University of Michigan, Ann Arbor, MI, 48109, USA

Sputter erosion of boron nitride (BN) is a critically important process in Hall thrusters from the point of view of both lifetime assessment and contamination effects. This contribution describes recent improvements to a laser sensor being developed for *in situ* monitoring of sputtered BN from Hall thrusters. The sensor employs the continuous-wave cavity ring-down spectroscopy (cw-CRDS) technique to probe an atomic absorption line of boron (250 nm). Recent improvements include piezo-electric cavity modulation, improved ring-down acquisition rate, and a custom AOM driver. We present demonstrative results illustrating these improvements and discuss their implications for Hall thruster diagnostics. A factor of ~ 5 improvement in optical sensitivity is demonstrated compared to the previous sensor.

Nomenclature

Abs	= optical absorbance
c	= speed of light in vacuum
d	= absorption sample length
f	= ring-down ingestion rate
$k(\nu)$	= absorption coefficient
l	= optical cavity length
L_c	= single-pass empty cavity loss
R	= reflectivity of cavity mirror
τ	= 1/e decay time, ring-down time
τ_o	= 1/e decay time of empty or detuned cavity
$\Delta\tau$	= standard deviation of ensemble of ring downs
S	= optical sensitivity

*Graduate Student, Physics, blee66@rams.colostate.edu

[†]Ph. D., Mechanical Engineering, ltao@princeton.edu

[‡]Research Assistant, Mechanical Engineering, jtay@enr.colostate.edu

[§]Associate Professor, Mechanical Engineering, ayalin@enr.colostate.edu

[¶]Professor, Aerospace Engineering, rasta@umich.edu

I. Introduction

PROPULSION systems with high exhaust velocities and long lifetimes are desirable for long-term space missions such as satellite station keeping or more imaginative deep-space missions. Buoyed by the success of ion thruster technology on Deep Space 1, interest in electric propulsion thrusters has continued to grow. Studies have shown that orbit transfer missions of interest to NASA may require a characteristic velocity increment of over 6 km/s.¹ Hall effect thrusters have specific impulses in excess of 1500 seconds with xenon propellant, which is far greater than impulses closer to 400 seconds generated from chemical systems.¹ Despite having higher propellant efficiency, the total thrust provided is low, requiring long-term operation to achieve the needed delta-V. Clearly, long engine lifetime is critical for such missions, which often require the engines to operate for thousands of hours without failure. Electric propulsion drives have the potential to meet these needs.

The primary life-limiting factor for Hall thrusters is sputter erosion of the insulator channel, typically formed from boron nitride (BN). Sputter erosion occurs when ions from the plasma contained within the thruster strike the channel wall, ejecting particles from the surface. Eventually the wall material is completely eroded, exposing the underlying magnetic components, and leading to end of life. Another very serious problem posed by sputtering is the deposition of the sputter products² (exiting from the exhaust plume) on sensitive spacecraft elements, e.g. solar panels or sensors, which can lead to malfunctions or spacecraft failure.

Currently, the most common testing method for Hall thruster lifetime is full-life testing. In these tests, the thruster is operated in a vacuum chamber for a duration exceeding that of the targeted mission. For example, a BPT-4000 Hall Thruster was operated for 10,400 hours at the Jet Propulsion Laboratory (JPL) as part of the engines flight qualification process.³⁻⁵ The NEXT thruster currently holds the record for the longest operating duration of any ion or Hall thruster, as it has surpassed 30,352 hours of testing.⁶ Though a careful means of ensuring adequate thruster life, thruster life tests suffer from various shortcomings. They are both expensive and intensive, tying up vacuum facilities and engineers for years. The process only yields information after test completion, thereby prohibiting real-time measurements and restricting the test to a single operating condition. It would be beneficial, for example, to understand how the erosion rate changed with operation time. Additionally, bulk erosion analysis does not give detailed information about the velocity of the ejected particles, which would be useful in validating (or seeding) numeric models.^{7,8}

What is needed, therefore, is a method for measuring thruster erosion rates non-intrusively, in real- or near-real-time, and which provides detailed information on the spatial distribution of eroded thruster material in the plume. Optical emission spectroscopy has been used to make measurements of the relative wall erosion rate in a BHT-200 Hall thruster.⁹ While this technique observed the optical emission of atomic boron in the exhaust plume to give real-time measurements of the wall erosion rate, the results were only relative. Like many emission measurements, it is often impractical to relate these measurements to an absolute number density. Another diagnostic technique used multilayer chip coatings within the insulator material.¹⁰ These chips contained thin layers of marker materials, which when sputter eroded, caused unique emission signals in the exhaust plume. One of the drawbacks of this method is the need for a specially prepared Hall thruster in order to perform diagnostics, which not only adds time and cost, but leaves questions as to whether the alterations affect the thruster operation.

This contribution updates our ongoing development of a cavity ring-down spectroscopy (CRDS) sensor to study sputter erosion of BN. Our past research has shown the possibility of a near real-time sputter sensor for industrial ion beam etch systems,¹¹ as well as a CRDS sensor for detecting sputtered particles from an anode layer type thruster.¹² In comparison to the two aforementioned works, both of which probed manganese atoms (403 nm), the measurement scheme for sputtered BN is significantly more challenging as the needed absorption lines are in the ultraviolet (250 nm). Challenges with CRDS in the ultraviolet include lower cavity mirror reflectivity (and therefore poorer detection limits), a higher cost of obtaining a single-mode tunable laser as well as the difficulty of single-mode fiber optic delivery. As the first steps towards the needed sensor, we have previously demonstrated our ability to detect sputtered BN using a simpler and lower sensitivity pulsed laser setup,¹³ as well as a higher sensitivity version using continuous-wave (cw) CRDS.¹⁴ Our collaborators from the University of Michigan have recently used a parallel cw-CRDS system to perform measurements of BN erosion rates from a 6-kW Hall thruster.¹⁵ While their measurements gave interesting results, the uncertainties were quite high, thereby showing a need for improved sensor sensitivity. The present contribution describes sensitivity improvements to the cw-CRDS BN sensor, making it more appropriate for rapid *in situ* Hall thruster diagnostics. The improvements include an increased ring-down

acquisition rate, an improved fast optical switch, and better ring-down filtering.

The layout of the paper is as follows. Section 2 describes the diagnostic technique and optical detection scheme. Section 3 describes the experimental setup for the sensor. Demonstrative results and discussion of the improved sensor are given in section 4, and conclusions are presented in section 5.

II. Boron Nitride Detection Technique

A. Cavity Ring-Down Spectroscopy

Cavity ring-down spectroscopy is a direct absorption spectroscopy measurement technique that provides extremely high sensitivity by employing enhanced optical-path length.^{16,17} In CRDS, a high finesse optical cavity (resonator) is excited with a probing laser. The absorbing sample, in this case the sputter products in the plume of the thruster, is contained within the cavity. When the exciting laser is quickly extinguished, the intensity exiting the cavity will follow an exponential decay. The exponential decay time constant (also termed ring-down time), τ , is related to the total loss inside the cavity, which is due to the single-pass empty cavity loss L_c (dominated by mirror loss which is approximately equal to $1-R$), and sample absorbance $Abs(\nu)$:

$$\frac{1}{\tau(\nu)} = \frac{c}{l}(L_c + Abs(\nu)) = \frac{1}{\tau_o} + \frac{c}{l} \int_0^d k(x, \nu) dx \quad (1)$$

where c is the speed of light, ν is the laser frequency, l and d are the cavity length and the sample length respectively, x is the position along the optical axis, $k(x, \nu)$ is the absorption coefficient, and τ_o is empty cavity ring-down time (often measured by detuning the laser from the sample absorption). In many spectral regions, mirror reflectivities in excess of 99.99% are available. This results in effective absorption path lengths of several kilometers.

There are primarily three factors which determine the optical sensitivity of a CRDS sensor: the inherent mirror loss, the noise in the ring-down time, and the ingestion rate (number of ring-downs recorded in a given time period). They combine to give an optical sensitivity of

$$S = \frac{1(1-R)\Delta\tau}{d\sqrt{f}\tau} \quad (2)$$

where R is the cavity mirror reflectivity, f is the ring-down ingestion rate, $\Delta\tau$ is the $(1-\sigma)$ standard deviation of an ensemble of ring-downs and τ is the average ring-down time for that ensemble. This is a measure of the optical sensitivity in units of $\text{cm}^{-1} \text{Hz}^{-1/2}$, which is proportional to, but different from a number density detection limit. Also note the difference between the length of the absorbing sample, d , and the physical cavity length, l . One cannot improve the sensor sensitivity by simply making the cavity longer unless the sample of interest also scales in length.

B. Boron Nitride Detection Scheme

Although the insulating channel of the Hall thruster is made of BN, the sputter products are typically ejected as atomic boron and nitrogen.¹⁸ Absorption lines for atomic nitrogen are in the vacuum ultraviolet and we elect to measure atomic boron, which directly relates to the amount of sputtered BN. A partial energy level diagram for neutral boron (B I) is shown in Fig. 1. The ground term has two distinct levels: $2s^2P_{1/2}^0$ (0 eV) and $2s^2P_{3/2}^0$ (0.00189 eV). As a result, fine-structure splitting results in two distinct boron absorption lines near 250 nm: the $2s^2P_{1/2}^0 \rightarrow 3s^2S_{1/2}$ transition at 249.753 nm, and the $2s^2P_{3/2}^0 \rightarrow 3s^2S_{1/2}$ transition at 249.848 nm. These lines are selected for CRDS measurement based on their optical accessibility and high absorption strength. From the energy level information of boron atoms and partition function, more than 99.9% of all boron atoms

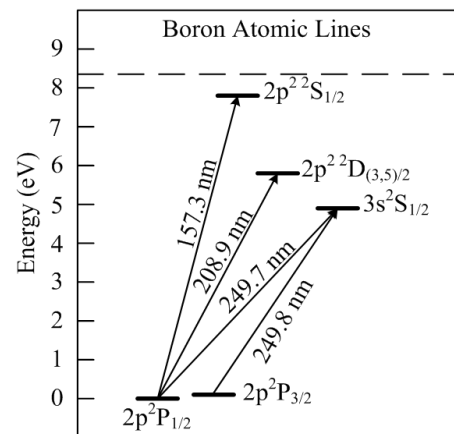


Figure 1. Partial energy diagram for atomic boron.

population is calculated to reside in the split ground state (66.6% of all population in $2s^2P_{3/2}^0$). Therefore, we chose the line at 249.848 nm for detection of atomic boron.

III. Experimental Setup

A. Optical Apparatus

The demonstrative measurements reported here were all performed on a table-top setup (i.e. not within a vacuum chamber). Fig. 2 shows the setup for this apparatus. The ultraviolet light used for boron detection is generated by a frequency-quadrupled external-cavity diode laser (Toptica TA-FHG110) producing about 15 mW of power at 250 nm. An acousto-optic modulator (AOM, Neos Technologies) was used as a fast optical switch, the details of which will be given later. The first order diffracted beam from the AOM was used to excite optical cavity. The diffracted beam from the AOM is sent through a mode match telescope and a pinhole. The pinhole acts as a spatial filter, ideally only allowing the Gaussian mode to transmit while the lens pair acts to match that Gaussian mode to the cavity. A 75 cm long stable optical cavity is formed by a pair of high reflective mirrors ($R=99.75\%$, MLD Technologies), both having a radius of curvature of 1 m. A piezoelectric stack (PZT) is attached to the output mirror of the cavity. This is used to modulate the cavity length a distance of ~ 1.1 free spectral ranges (FSR), thereby ensuring that at least one cavity resonance is excited for each sweep of the PZT. The cavity output is sent to a photo-multiplier tube (PMT, Hamamatsu R9110) which converts the optical signal to a voltage signal to be read by the data acquisition system (details given later). An interference filter (Edmund Optics, NT67-809) centered at 248 nm with a 40 nm FWHM bandwidth is used to reject unwanted light from the PMT. The filter has a transmission of 20% at the wavelength of interest, and a suppression of $\sim 10^{-4}$ outside the bandpass.

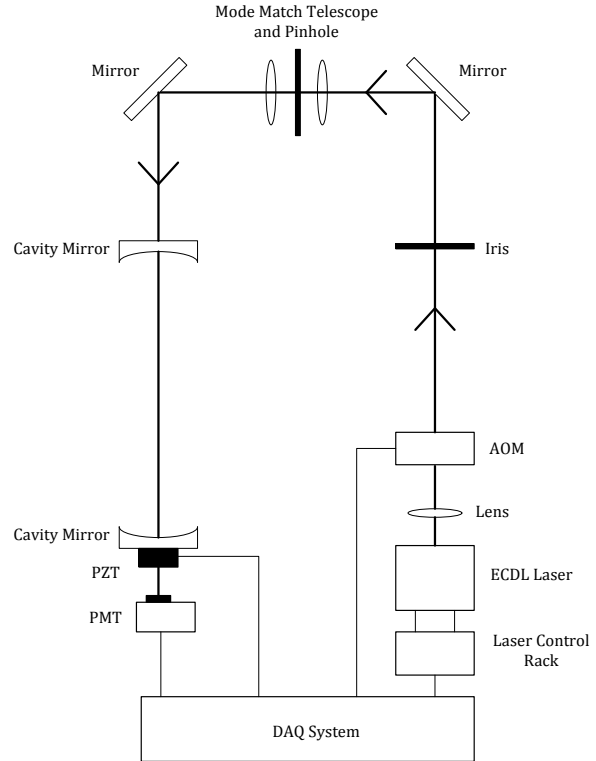


Figure 2. Optical apparatus for table-top tests of CRDS at 250 nm.

B. Data Acquisition and Control System

One of the major changes to the CRDS sensor was an upgrade of the data acquisition (DAQ) system. With the addition of the PZT to modulate the cavity, the system's ability to generate ring-downs quickly is greatly increased. Given the relatively low reflectivity of mirrors at 250 nm, the resonances of the cavity can be excited with high injection efficiency even when the cavity is modulated at many hundreds of times a second. This places a higher demand on the speed of the DAQ system. In cw-CRDS, the system electronics need to be able to detect a resonance, quickly extinguish the optical switch, digitize and record the decay signal and, in our case, perform fitting and filtering of the signal.

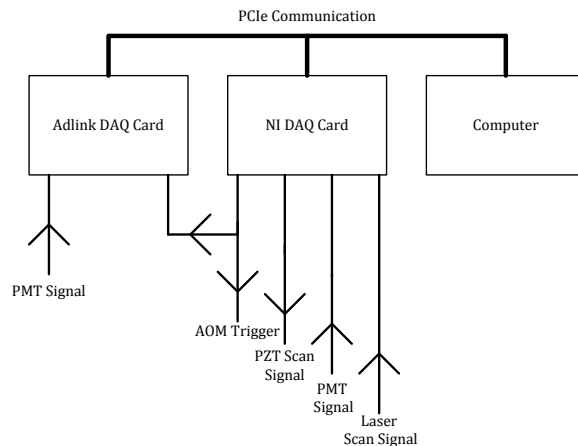


Figure 3. Diagram of the DAQ system.

in real time. This was previously accomplished with a mixture of custom circuits, oscilloscopes and computers. The present work uses only a desktop computer for triggering, signal acquisition, PZT control, and frequency calibration. This system is diagramed in Fig. 3.

The decay signals from the PMT are digitized at a rate of 200 MHz by a 14-bit PCIe digitizing card (Adlink PCIe-9842). Triggering of the digitizing card and AOM, scanning of the PZT and frequency calibration are all performed by a multipurpose PCIe DAQ card (National Instruments PCIe-6351). The triggering circuit within this card is capable of reacting to a resonance within about 20 ns, with a minimum delay of 20 ns between triggers. The delay in extinguishing the optical signal is still dominated by the propagation delay of the acoustic wave within the AOM itself. This triggering method also allows for the triggering parameters to be changed much more easily than if a custom circuit were used. A custom written Labview program controls both of these cards and performs the real-time data analysis. The system is capable of handling ring downs at over 1 kHz (including separately fitting and filtering each ring-down in real-time).

Utilizing PCIe communication and a high speed CPU (Intel 2600K) were both important in achieving this speed. The digitizing cards ability to retrigger quickly may be a severely limiting factor in the ring-down ingestion rate. Also, being that Labview is an interpreted programming language, it is known to be relatively slow. Further speed may be gained by writing the control and analysis programs directly in a compiled language like C.

C. Custom AOM Driver

Beam diffraction occurs within the AOM because a transducer attached to the AOM crystal uses an RF signal to excite lattice vibrations. The RF signal is generated by the AOM driver, which consists of an oscillator, a switch and an amplifier. A key parameter for CRDS is the extinction ratio of the AOM.¹⁹ The extinction ratio is the ratio of the power when the AOM is off versus on. Power may refer to either the RF electrical power being sent to the AOM, or the optical power in the first order diffracted beam. If this ratio is not sufficiently low, residual light will continue to excite the cavity even after the AOM is off. This results in instabilities in the ring-down signal, thereby increasing $\Delta\tau$.

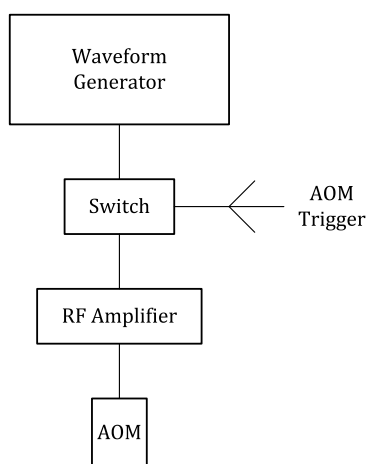


Figure 4. Custom RF driver diagram for AOM.

Originally, the AOM used in the BN CRDS sensor was matched with a pre-packed AOM driver from Neos Technologies. The driver gave an extinction ratio in the optical power of -41 dB. Although -41 dB is a fairly good isolation, it will be seen in section 4 that this residual light causes an increase in $\Delta\tau$. To improve this, a custom AOM driver was used, as shown in Fig. 4. The 110 MHz sine signal was initially generated by an arbitrary function generator (Tektronix AFG 3252). A fast RF switch (Minicircuits ZASWA-2-50DR+) is used to block the RF signal once a trigger signal is received. This switch has a minimum RF power isolation of -75 dB at this frequency. The RF signal is finally sent through an RF amplifier (Empower 1063-BBM0D3FAJ) and is amplified to the needed 2 W of electrical power before being sent to the AOM. The spurious RF levels emanating from the amplifier are below -60 dBc (-60 dB relative to the RF input). This system gives an extinction ratio in optical power of -48 dB. Although this is only a small improvement to the extinction ratio, it yielded a notable decrease in $\Delta\tau$, as will be shown later. From the work by Huang et al., RF extinction ratios below about -65 dB will not further decrease the ring-

down noise. Given that the custom driver is close to this ratio, we do not expect large improvements by using a lower extinction ratio driver.

D. Ring-Down Fitting and Filtering

In principle, at a fixed laser frequency, there is no need to individually fit each ring-down signal. One could collect many decay events, average the signal and fit the result. The flaw with this method is that, in practice, not all of the collected ring downs will be ‘good.’ The signal may have saturated the detector or the digitizer, the signal peak at the beginning of the decay may be very low (despite enforcing a minimum trigger level), or, as has been seen with our digitizer, the data may have occasional artifacts resulting from

data read errors. It is therefore desirable to fit each decay individually, and to use filters to exclude ‘bad’ ring downs.

Three filters are imposed in our system. First, if the peak voltage of the signal is not at least $\sim 50\%$ of the maximum digitizer voltage, the ring down is ignored. Second, if the peak voltage of the signal is identically 100% of the maximum voltage (i.e. either the detector or digitizer is saturated), then individual data points are removed from the beginning of the decay until the voltage is no longer saturated. If both of these tests are passed, the ring down will be fit. Once the fit parameters are determined, the reduced χ^2 for the fit is computed. Ideally, this value should be close to one. However, this value could be higher because of data read errors, electrical noise spikes or any number of other reasons. If the reduced χ^2 exceeds a pre-set value, the ring down will be ignored.

IV. Results and Discussion

Demonstrative measurements were made to assess the optical sensitivity of the improved system, which can be compared to previous versions of the BN sensor. Previous table-top tests at both CSU and UM had ingestion rates of 50-150 Hz, $\Delta\tau/\tau$ values of $\sim 1\%$, a cavity length of 90 cm, and empty cavity ring-down times of $\sim 1 \mu s$. Note that during sputtering experiments ring-down times tend to drop due to contamination effects.¹⁵ These parameters give a sensitivity of $S \approx 2.3 \times 10^{-8} \text{ cm}^{-1} \text{ Hz}^{-1/2}$. Through the various improvements described below, this has been decreased to $S \approx 5.1 \times 10^{-9} \text{ cm}^{-1} \text{ Hz}^{-1/2}$. We can also compare this to a pulsed-CRDS system operating at a similar wavelength,²⁰ which operated at $S \approx 1.9 \times 10^{-8} \text{ cm}^{-1} \text{ Hz}^{-1/2}$.

A. Ingestion Rate Benchmarks

There were several limitations to the ingestion rate of the previous sensor version. The external-cavity diode laser used is capable of scanning many GHz by sweeping the cavity diffraction grating. The system previously used a fixed cavity to sweep the laser over the cavity resonances. Scanning in this fashion was limiting because the laser would become unstable or have reduced output power at high scan speeds. Also, slower software, DAQ cards and computers were used. Combined, these problems placed an upper limit on the ingestion rate of ~ 150 Hz or less.

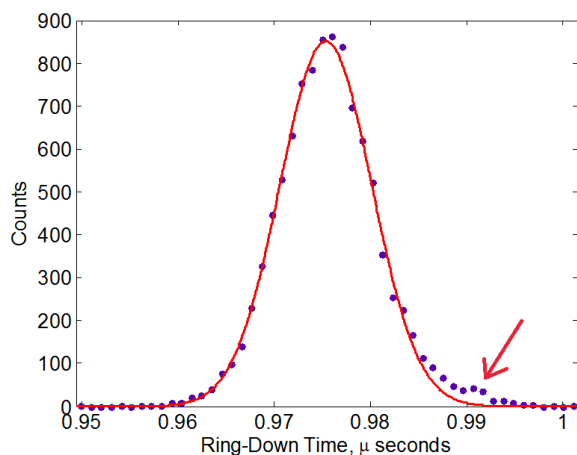


Figure 5. A histogram of ring-down times from 10,000 ring-down signals which passed filtering. The red line is a fit to a Gaussian. The small peak near $0.99 \mu s$ is caused by higher order modes.

After filtering, a sustained ingestion rate of 700 ‘good’ ring-downs per second was achieved. Due to the increased variance in the resonance amplitude mentioned earlier, the filter which usually failed was the minimum signal strength condition. Since CRDS sensitivity scales as the square root of ingestion rate, an increase from 150 to 700 Hz netted more than a factor of 2 improvement.

The PZT in the improved sensor was scanned in a triangle wave with a voltage amplitude corresponding to ~ 1.1 FSRs with a frequency between 300 and 500 Hz (note that in each period, the PZT will pass a resonance twice). At these higher scan speeds, the mean optical signal hitting the detector when the laser and cavity are on resonance decreases and the variance increases.²¹ In order to reliably trigger on the majority of the resonances, a higher PMT gain is needed. Since the PMT noise does not noticeably scale with gain in the needed gain range, this results in a negligible noise increase in each ring down. Due to the higher peak variance and increased PMT gain, more higher order modes were triggered than normal, as shown in Fig. 5. The small peak near $0.99 \mu s$ is a result of higher order modes being triggered and fit, however the increase in $\Delta\tau$ was negligible.

A typical ingestion rate was 800-1000 Hz, however, many of these ring downs did not pass the filters mentioned earlier.

B. Improved AOM Extinction Ratio

As mentioned before, by using a custom RF generator to drive the AOM, the optical extinction ratio increased from -41 dB to -48 dB. The values of $\Delta\tau/\tau$ for these cases were 0.8% and 0.4% respectively (taken for an ensemble of 5000 ring downs). This is roughly commensurate with the noise versus extinction ratio plot given in the work by Huang and Lehmann.¹⁹ As the authors explain, the finite extinction ratio of the excitation beam typically manifests itself as a reduced χ^2 value higher than 1. The increased χ^2 value is caused by higher signal variance in the beginning of the ring down as compared to the tail of the decay signal where the data variance is measured, which can also be seen in fit residues, examples of which are given in Fig. 6. The residues have a zero mean, therefore Fig. 6 shows rms residues which were averaged for 7 ring-down signals. For the two ensembles of ring downs mentioned above, the mean reduced χ^2 value decreased from 1.77 to 1.55 by using the custom AOM driver. Histograms for these values are shown in Fig. 7.

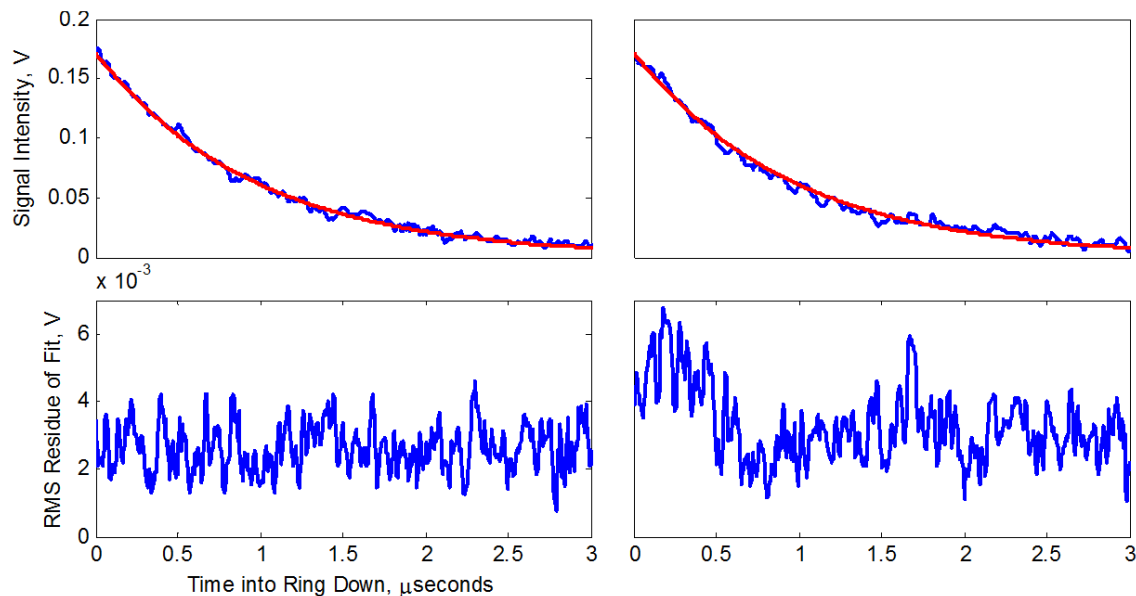


Figure 6. Examples of ring-down signals with exponential fits (top) and associated averaged RMS fit residues (bottom) for the custom AOM driver (left) compared to the pre-packaged AOM driver (right).

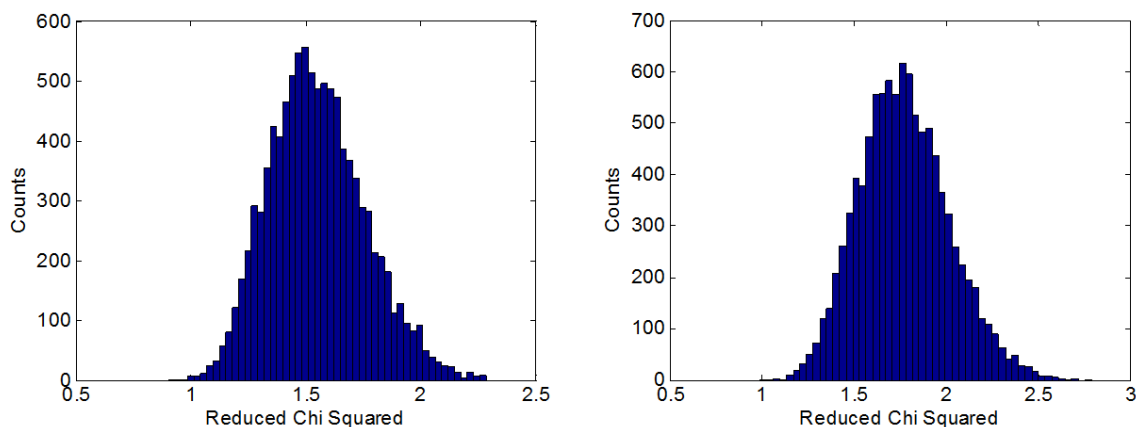


Figure 7. Reduced chi squared values for custom AOM driver (left) and the pre-packaged AOM driver (right).

C. Sensitivity Benchmarks

Two benchmark measurements were performed to assess the optical sensitivity of the improved BN sensor. First, an ensemble of 5,000 ring downs were measured. This experiment gave an average τ of $0.98 \mu\text{s}$, $\Delta\tau/\tau$

of 0.4%, and an average ingestion rate of 714 Hz (only counting ring downs which passed the filters). Using Eq. 2, this results in a sensitivity of $S \approx 5.1 \times 10^{-9} \text{ cm}^{-1} \text{ Hz}^{-1/2}$.

To test the system’s ability to increase precision by operating for longer periods of time, ring downs were recorded for 1 hour and the standard error of the mean in τ was calculated and is displayed in Fig. 8. These results show the system possesses the needed stability to capitalize on prolonged averaging. It should be noted, however, that operating within a vacuum facility next to a Hall thruster may induce considerably more drift in τ than was observed in the table-top setup.

It is also of interest to relate the optical sensitivity quoted above to a limit of detection for atomic boron. This comparison is given below in Table 1. Typical boron densities integrated over an absorption path length of $\sim 10 \text{ cm}$ are $10^9 - 10^{10} \text{ cm}^{-2}$.²² An approximate conversion is that a line integrated boron density of 10^9 cm^{-2} gives an optical absorbance of 10 ppm. Using Eqn. (2) and assuming an integration time of 10 seconds gives a unitless optical limit of detection, which is given in Table 1.

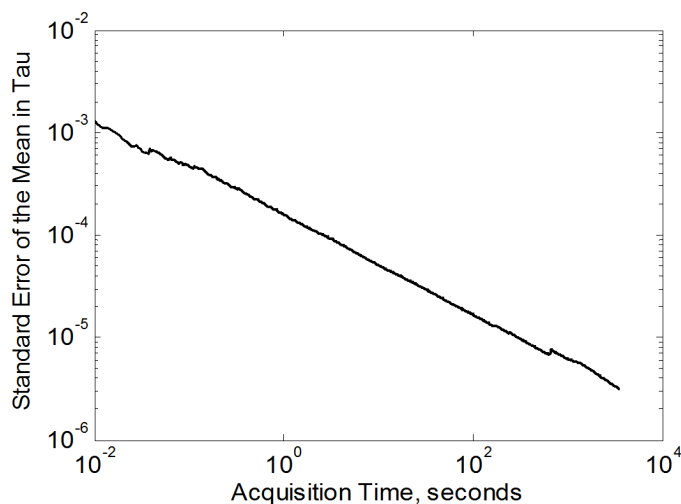


Figure 8. Standard error of the mean in ring-down time for a 1 hour integration time.

Table 1. Optical sensitivity to boron number density comparison for 10 second integration time.

	Absorbance Limit of Detection (ppm)	S:N for 10^9 cm^{-2} boron	10^{10} cm^{-2} boron
Lei et al. Sensor ¹⁴	2.3	4.3	43
Current Sensor	0.5	20	200

V. Conclusion

We have demonstrated a factor of ~ 5 improvement in optical sensitivity relative to past implementations of the BN CRDS sensor. These improvements were accomplished primarily with a significant increase in ring-down ingestion rate along with an improved extinction ratio in the optical switch. We have also demonstrated the system’s ability to perform prolonged averaging in a table-top environment. The improvement in optical sensitivity directly translates into the same increase in signal to noise ratio for Hall thruster diagnostics.

Acknowledgments

The authors would like to thank the research group of Dr. Jacob Roberts in the CSU Physics Department for their generous loan of RF equipment.

References

- ¹Gulczinski, F. and Spores, R., "Analysis of Hall-Effect Thrusters and Ion Engines for Orbit Transfer Missions," *32nd Joint Propulsion Conference*, Vol. AIAA-96-2973, 1996.
- ²Mahan, J. E. and Vantomme, A., "Trends in sputter yield data in the film deposition regime," *Physical Review B*, Vol. 61, No. 12, 2000, pp. 8516-8525.
- ³Hofer, R., "High-Specific Impulse Operation of the BPT-4000 Hall Thruster for NASA Science Missions," *46th Joint Propulsion Conference*, Vol. AIAA 2010-6623, Nashville, TN, 2010.
- ⁴Grys, K., Mathers, A., and Welander, B., "Demonstration of 10,400 Hours of Operation on a 4.5 kW Qualification Model Hall Thruster," *46th Joint Propulsion Conference*, Vol. AIAA 2010-6698, Nashville, TN, 2010.
- ⁵Mikellides, I., Katz, I., Hofer, R., and Goebel, D., "Magnetic Shielding of the Acceleration Channel Walls in a Long-Life Hall Thruster," *46th Joint Propulsion Conference*, Vol. AIAA 2010-6942, Nashville, TN, 2010.
- ⁶Herman, D., "Status of the NASA's Evolutionary Xenon Thruster (NEXT) Long-Duration Test after 30,352 Hours of Operation," *46th Joint Propulsion Conference*, Vol. AIAA 2010-7112, Nashville, TN, 2010.
- ⁷Cheng, S. and Martinez-Sanchez, M., "Modeling of Hall thruster lifetime and erosion mechanisms," *30th International Electric Propulsion Conference*, Vol. IEPC-2007-250, Florence, Italy, 2007.
- ⁸Yim, J. and Boyd, I., "Hall Thruster Erosion Prediction Using a Hydrodynamic Plasma Model and Sputtering Simulation," *30th International Electric Propulsion Conference*, Vol. IEPC-2007-34, Florence, Italy, 2007.
- ⁹Celik, M., Batishchev, O., and Martinez-Sanchez, M., "Use of emission spectroscopy for real-time assessment of relative wall erosion rate of BHT-200 hall thruster for various regimes of operation," *Vacuum*, Vol. 84, No. 9, 2010, pp. 1085-1091.
- ¹⁰Cho, S., Yokota, S., Hara, K., and Takahashi, D., "Hall Thruster Channel Wall Erosion Rate Measurement Method Using Multilayer Coating Chip," *46th Joint Propulsion Conference*, Vol. AIAA 2010-6697, Nashville, TN, 2010.
- ¹¹Tao, L., Yalin, A. P., and Yamamoto, N., "Cavity ring-down spectroscopy sensor for ion beam etch monitoring and end-point detection of multilayer structures," *Review of Scientific Instruments*, Vol. 79, No. 11, 2008.
- ¹²Yamamoto, N., Tao, L., Rubin, B., Williams, J. D., and Yalin, A. P., "Sputter Erosion Sensor for Anode Layer-Type Hall Thrusters Using Cavity Ring-Down Spectroscopy," *Journal of Propulsion and Power*, Vol. 26, No. 1, 2010, pp. 142-148.
- ¹³Yalin, A., Surla, V., Tao, L., Smith, T., and Gallimore, A., "Boron Nitride Sputter Erosion Measurements by Cavity Ring-Down Spectroscopy," *30th International Electric Propulsion Conference*, Vol. IEPC-2007-075, Florence, Italy, 2007.
- ¹⁴Tao, L., Lee, B., Yamamoto, N., Gallimore, A., and Yalin, A., "Development of a Cavity Ring-Down Spectroscopy Sensor for Boron Nitride Erosion in Hall Thrusters," *31st International Electric Propulsion Conference*, Vol. IEPC-2009-146, Ann Arbor, MI, 2009.
- ¹⁵Huang, W., Gallimore, A., and Smith, T., "The Technical Challenges of using Cavity Ring-Down Spectroscopy to Study Hall Thruster Channel Erosion," *32nd International Electric Propulsion Conference*, Vol. IEPC-2011-030, Weisbaden, Germany, 2011.
- ¹⁶Berden, G., Peeters, R., and Meijer, G., "Cavity ring-down spectroscopy: Experimental schemes and applications," *International Reviews in Physical Chemistry*, Vol. 19, No. 4, 2000, pp. 565-607.
- ¹⁷Paldus, B. A. and Kachanov, A. A., "An historical overview of cavity-enhanced methods," *Canadian Journal of Physics*, Vol. 83, No. 10, 2005, pp. 975-999.
- ¹⁸Rubin, B., Topper, J. L., and Yalin, A. P., "Total and differential sputter yields of boron nitride measured by quartz crystal microbalance," *Journal of Physics D-Applied Physics*, Vol. 42, No. 20, 2009.
- ¹⁹Huang, H. and Lehmann, K., "Noise caused by a finite extinction ratio of the light modulator in CW cavity ring-down spectroscopy," *Applied Physics B-Lasers and Optics*, Vol. 94, No. 2, 2009, pp. 355-366.
- ²⁰Fain, X., Moosmuller, H., and Obrist, D., "Toward real-time measurement of atmospheric mercury concentrations using cavity ring-down spectroscopy," *Atmospheric Chemistry and Physics*, Vol. 10, No. 6, 2010, pp. 2879-2892.
- ²¹Morville, J., Romanini, D., Chenevier, M., and Kachanov, A., "Effects of laser phase noise on the injection of a high-finesse cavity," *Applied Optics*, Vol. 41, 2002, pp. 6980-90.
- ²²Yalin, A., Tao, L., Sullenderger, R., Oya, M., Yamamoto, N., Smith, T., and Gallimore, A., "High-Sensitivity Boron Nitride Sputter Erosion Measurements by Continuous-Wave Cavity Ring-Down Spectroscopy," *44th Joint Propulsion Conference*, Vol. AIAA-2008-5091, Hartford, CT, 2008.